

# Non-Markovian quantum exceptional points

Received: 2 July 2024

Accepted: 13 January 2025

Published online: 03 February 2025

 Check for updates

Jhen-Dong Lin <sup>1,2,8</sup>, Po-Chen Kuo <sup>1,2,8</sup>, Neill Lambert <sup>3,4</sup>,  
Adam Miranowicz <sup>3,5</sup>, Franco Nori <sup>3,4,6</sup>  & Yueh-Nan Chen <sup>1,2,7</sup> 

Exceptional points (EPs) are singularities in the spectra of non-Hermitian operators where eigenvalues and eigenvectors coalesce. Open quantum systems have recently been explored as EP testbeds due to their non-Hermitian nature. However, most studies focus on the Markovian limit, leaving a gap in understanding EPs in the non-Markovian regime. This work addresses this gap by proposing a general framework based on two numerically exact descriptions of non-Markovian dynamics: the pseudomode equation of motion (PMEOM) and the hierarchical equations of motion (HEOM). The PMEOM is particularly useful due to its Lindblad-type structure, aligning with previous studies in the Markovian regime while offering deeper insights into EP identification. This framework incorporates non-Markovian effects through auxiliary degrees of freedom, enabling the discovery of additional or higher-order EPs that are inaccessible in the Markovian regime. We demonstrate the utility of this approach using the spin-boson model and linear bosonic systems.

Spectral singularities for non-Hermitian systems, known as exceptional points (EPs), have attracted intense research attention over the past decades<sup>1–4</sup>. These singularities are pivotal in studying open systems, as environmental noise inherently breaks the Hermiticity. Early studies of EPs mainly focused on non-Hermitian Hamiltonians (NHHs)<sup>5–7</sup> that are suitable for modeling classical and semiclassical systems. In these settings, (semi-)classical EPs, often termed Hamiltonian EPs (HEPs), are identified by the convergence of at least two eigenvalues and their corresponding eigenstates within NHHs. Notably, it has been shown that environmental noises can induce exotic effects near HEPs, e.g., EP-induced lasing<sup>8–10</sup>, programmable mode switching<sup>11</sup>, and EP-enhanced sensitivity<sup>12–16</sup>.


Recently, investigations of EPs have extended into the full quantum regime<sup>17–30</sup>, where the temporal evolution of an open quantum system is governed by a Lindblad master equation or, equivalently, by a Liouvillian superoperator. Unlike the effective NHHs, Liouvillian superoperators incorporate the concept of quantum jumps into the dynamical process<sup>31</sup>. In this context, the EPs associated with Liouvillian superoperators are termed quantum EPs or Liouvillian EPs (LEPs).

It has been demonstrated that pure quantum EPs exist<sup>17</sup>, which are phenomena without (semi-)classical counterparts.

To date, the exploration for both HEPs and LEPs has largely been confined to the Born-Markov-Secular (BMS) approximation, which is only valid in cases of sufficiently weak system-environment interaction or environments without any structure. Recently, several works have indicated that EP-like critical behaviors<sup>32–37</sup> could manifest in the non-Markovian regime. However, whether the concepts of LEPs can be directly generalized to the non-Markovian regime remains an open question. A primary challenge lies within the structure of the non-Markovian equation of motion for reduced dynamics, which can be generally expressed as:

$$\frac{d\rho_S(t)}{dt} = \int_0^t d\tau \mathcal{K}(t, \tau) \rho_S(\tau). \quad (1)$$

Here, the non-Markovian effect is encoded in the memory kernel  $\mathcal{K}(t, \tau)$ <sup>31</sup>, and  $\rho_S(t)$  denotes the open system's reduced density operator. The integral-differential nature of this time-non-local equation

<sup>1</sup>Department of Physics, National Cheng Kung University, Tainan 701, Taiwan. <sup>2</sup>Center for Quantum Frontiers of Research & Technology, NCKU, Tainan 701, Taiwan. <sup>3</sup>Theoretical Quantum Physics Laboratory, Cluster for Pioneering Research, RIKEN, Wakoshi, Saitama 351-0198, Japan. <sup>4</sup>Center for Quantum Computing, RIKEN, Wakoshi, Saitama 351-0198, Japan. <sup>5</sup>Institute of Spintronics and Quantum Information, Faculty of Physics and Astronomy, Adam Mickiewicz University, 61-614 Poznań, Poland. <sup>6</sup>Quantum Research Institute, The University of Michigan, Ann Arbor 48109-1040 MI, USA. <sup>7</sup>Physics Division, National Center for Theoretical Sciences, Taipei 106319, Taiwan. <sup>8</sup>These authors contributed equally: Jhen-Dong Lin, Po-Chen Kuo.  e-mail: [fnori@riken.jp](mailto:fnori@riken.jp); [yuehnan@mail.ncku.edu.tw](mailto:yuehnan@mail.ncku.edu.tw)

complicates the application of traditional spectral analysis techniques for identifying EPs.

In this work, we aim to address this theoretical gap. The main result lies in the development of a systematic framework for quantum EPs associated with generic non-Markovian open systems. The idea is based on applying the pseudomode equation of motion (PMEOM)<sup>38–48</sup> and the hierarchical equations of motion (HEOM)<sup>49–58</sup>, which can be used to describe a large class of system-environment models. In contrast to the memory kernel approach, as described in Eq. (1), the dynamics are governed by what we call extended Liouvillian superoperators, enabling us to perform conventional spectral analysis, identifying the corresponding EPs, and revealing their impacts on the non-Markovian open quantum systems. In other words, this approach is highly compatible with previous studies on LEPs. Further, the proposed framework can be viewed as a unified method for investigating both Markovian and non-Markovian quantum EPs, as the PMEOM and HEOM are exact descriptions of open quantum systems, making them applicable across all regimes.

An intriguing implication of this framework is that additional EPs may arise beyond the Markovian regime. This builds upon a distinctive feature of the PMEOM and HEOM: non-Markovian effects are captured by auxiliary degrees of freedom, specifically pseudomodes (PMs) and auxiliary density operators (ADOs). Consequently, the dimension of the extended Liouvillian superoperator generally exceeds that of the standard Liouvillian superoperator under the BMS approximation, thereby providing a greater capacity for establishing degeneracies.

Moreover, this dimension extension through the PMs or ADOs suggests a potential for generating higher-order EPs, which is a crucial topic due to their ability to induce ultra-sensitivity. Implementations of such higher-order EPs typically require scaling up the physical size of the open system<sup>13,59–63</sup>. However, the PMs and ADOs are introduced to effectively emulate the environmental influence on the system that may not directly correspond to the physical degrees of freedom of the environment. This presents an alternative route to achieving higher-order EPs by engineering non-Markovian reservoirs without the need to enlarge the open system.

Although the PMEOM and HEOM are equivalent in describing the exact dynamics, we will focus more on the former approach. This is because the PMEOM offers more physical intuition for identifying EP criteria by balancing the system-PM coupling and PM damping.

To demonstrate the aforementioned utility, we consider two analytically tractable examples. The first one is the spin-boson model with a

Lorentzian environment. We identify an emergent EP that cannot be observed in the Markovian wide-band limit, where the dynamics can be reduced to a BMS master equation. Intriguingly, the EP precisely aligns with the Markovian-to-non-Markovian transition, suggesting a possible relationship between the onset of non-Markovian information backflow and the non-Hermitian phase transition. In addition, we show that the EP criterion is tunable by reservoir engineering. Specifically, we introduce a band gap to the Lorentzian environment, demonstrating that the corresponding EP condition requires a smaller system-environment coupling strength compared to the gap-less scenario.

For the second example, we examine linear bosonic systems by using the adjoint PMEOM within the Heisenberg picture. We show that the dynamics of the modes' amplitudes can be determined by effective NHHs, enabling us to explore potential non-Markovian HEPs. As an example, we consider a two-coupled-modes system, where a second-order HEP emerges in the wide-band limit. We showcase that by reducing the spectral width, the HEP can be transformed to a third-order HEP. Consequently, the system becomes more sensitive to external perturbations with the help of the quantum memory effect. These findings reveal the intricate interplay between EPs and the memory effect, laying a theoretical foundation for exploring non-Hermitian physics toward non-Markovian and non-perturbative regimes.

## Results

### General framework for non-Markovian exceptional points

In this section, we present a general approach to characterize EPs for open systems subject to non-Markovian noise, as illustrated in Fig. 1. To begin with, we consider an open quantum system (S) coupled to a bosonic environment (E), where the total Hamiltonian is expressed by

$$H_{\text{tot}} = H_S + H_E + H_{SE} \text{ with } H_E = \sum_k \omega_k b_k^\dagger b_k, \quad (2)$$

$$H_{SE} = QX, \text{ and } X = \sum_k g_k (b_k^\dagger + b_k).$$

Here,  $H_S$  and  $H_E$  represent the free Hamiltonians of the system and its environment, while  $H_{SE}$  describes their interactions. Also,  $\omega_k$  and  $g_k$  correspond to the frequency and the coupling strength for the environmental mode  $b_k$ , respectively, and  $Q$  represents an arbitrary operator acting on the system that characterizes the system-environment coupling. We consider that the environment is initialized in a Gibbs state at temperature  $T$ :  $\rho_E = \exp(-\beta H_E)/\text{tr}[\exp(-\beta H_E)]$ ,

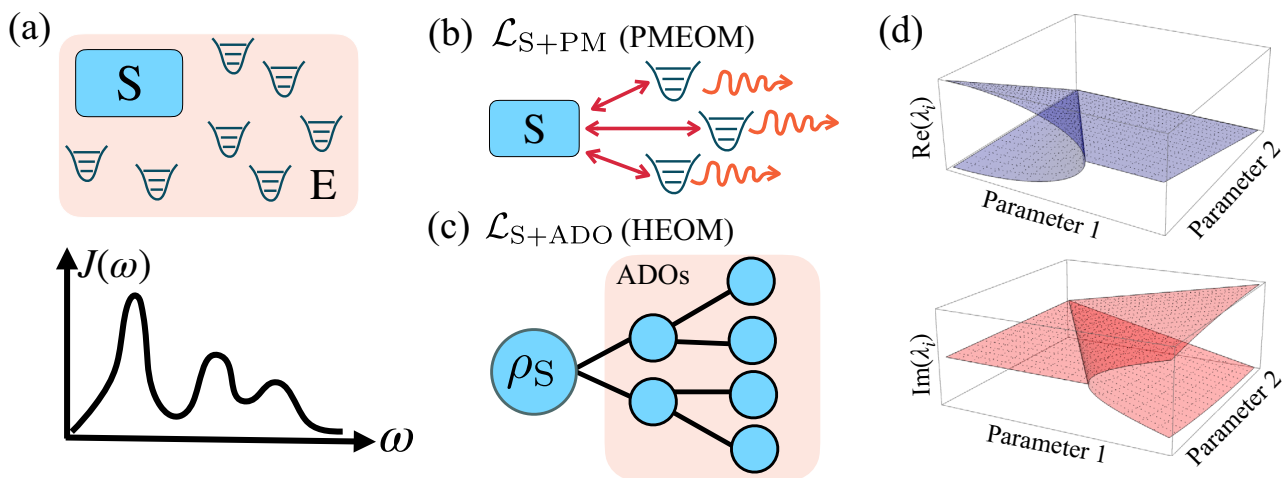


**Fig. 1 | Schematic illustration depicting EPs for a generic non-Markovian open-system model.** **a** Generic system-environment model where the structured environment is captured by the spectral density function  $J(\omega)$ . For a given spectral density function and the corresponding environmental correlation function, the exact non-Markovian dynamics can either be described by **b** the PMEOM or **c** the HEOM with the corresponding extended Liouvillian superoperators:  $\mathcal{L}_{S+PM}$  and  $\mathcal{L}_{S+ADO}$ . **d** The non-Markovian EPs can then be identified by observing the complex spectrum  $\{\lambda_i\}$  of these extended Liouvillian superoperators.

where  $\beta = (k_B T)^{-1}$  with  $k_B$  denoting the Boltzmann constant. In this case, the exact dynamics of the open system's reduced density matrix (within the interaction picture) can be written as

$$\rho_S(t) = \hat{T} \exp\{\hat{\mathcal{F}}[Q, C(t)]\} \rho_S(0). \quad (3)$$

Here,  $\hat{T}$  denotes the time-ordering operator and  $\hat{\mathcal{F}}$  represents the Feynman-Vernon influence functional<sup>31</sup>, which can be expressed by

$$\hat{\mathcal{F}} = - \int_0^t dt_1 \int_0^{t_1} dt_2 Q(t_1)^\times [C_{\mathbb{R}}(t_1 - t_2)Q(t_2)^\times + iC_{\mathbb{I}}(t_1 - t_2)Q(t_2)^\circ], \quad (4)$$

where  $Q(t) = \exp(iH_S t)Q \exp(-iH_S t)$ , and the superoperator notations  $Q(t)^\times = [Q(t), \bullet]$  and  $Q(t)^\circ = \{Q(t), \bullet\}$  denote the commutator and anti-commutator, respectively. In addition,  $C_{\mathbb{R}(\mathbb{I})}$  denotes the real (imaginary) part of the environmental correlation function

$$C(t) = \text{tr}[X(t)X(0)\rho_E], \quad (5)$$

with  $X(t) = \exp(iH_E t)X \exp(-iH_E t)$ . An essential feature of  $\hat{\mathcal{F}}$  is its exclusive dependence on the system-environment coupling operator  $Q$  and the environmental correlation function  $C(t)$ . The latter can be expressed by

$$C(t) = \int_0^\infty d\omega \frac{J(\omega)}{\pi} \left[ \coth\left(\frac{\beta\omega}{2}\right) \cos(\omega t) - i \sin(\omega t) \right], \quad (6)$$

where  $J(\omega) = \sum_k |g_k|^2 \delta(\omega - \omega_k)$  represents the coupling spectral density. This property enables the reproduction of the exact open system dynamics through an auxiliary model involving a small set of fictitious damping modes, i.e., the PMs, provided that the correlation function for the artificial model aligns with Eq. (6).

For a broad range of cases, the correlation function can be efficiently expressed as a finite weighted summation of exponential terms, i.e.,

$$C(t) = \sum_i \alpha_i^2 \exp(-i\Omega_i t - \gamma_i |t|/2). \quad (7)$$

This expression can be obtained by several approaches. For commonly used spectral densities, such as the Drude-Lorentz and Brownian motion types, analytical expressions for  $C(t)$  are available as an infinite sum of decaying exponentials (i.e., the Matsubara modes)<sup>54</sup>. In practice, this sum is truncated to balance accuracy with computational cost. More recently, the adaptive Antoulas-Anderson (AAA) algorithm<sup>64</sup>, a numerical subroutine, has been employed to optimize the underlying pole structure for the integration in Eq. (6), allowing for an efficient approximation of  $C(t)$  with a finite sum of exponentials<sup>65</sup>.

With this expression, one can construct the PMEOM:

$$\begin{aligned} \frac{d}{dt} \rho_{S+PM}(t) &= \mathcal{L}_{S+PM}[\rho_{S+PM}(t)] \\ &= -i[H_{S+PM}, \rho_{S+PM}(t)] + \sum_i \gamma_i \mathcal{L}_{a_i}[\rho_{S+PM}(t)], \end{aligned} \quad (8)$$

with  $H_{S+PM} = H_S + \sum_i \Omega_i a_i^\dagger a_i + \alpha_i Q(a_i^\dagger + a_i)$ ,

where,  $\{a_i\}$  represent the PMs, and we introduce the dissipator  $\mathcal{L}_{a_i}[\bullet] = a_i \bullet a_i^\dagger - \{a_i^\dagger a_i, \bullet\}/2$ . Notably, the environmental influences on the open system are now captured by the PMs' frequencies  $\Omega_i$ , damping rates  $\gamma_i$ , and the system-PM coupling strengths  $\alpha_i$ . The exact dynamics of  $S$  can be obtained by tracing out the PMs, i.e.,  $\rho_S(t) = \text{tr}_{PM}[\rho_{S+PM}(t)]$ , after solving the PMEOM with these PMs initialized in the thermal states.

One notable benefit of employing the PM model lies in its facilitation of establishing physical intuitions regarding the EP criteria. For instance, recent works have suggested that EPs are closely related to critical damping points for both classical and quantum systems<sup>22</sup>. As we demonstrate below, it is feasible to pinpoint EPs by balancing the system-PM coupling strength and the PM damping, leading the system to a critical damping point.

Furthermore, a systematic procedure for characterizing non-Markovian EPs based on a standard spectral analysis can be established. The main idea is grounded in the observation that both the temporal evolution of  $\rho_{S+PM}(t)$  and  $\rho_S(t)$  are governed by the spectral properties of the extended Liouvillian superoperator  $\mathcal{L}_{S+PM}$ . Specifically, assuming that  $\mathcal{L}_{S+PM}$  is diagonalizable, we consider its eigenvalues and the corresponding eigenmatrices:  $\{\lambda_i, \hat{\rho}_{S+PM,i}\}_i$ . The dynamics of  $\rho_{S+PM}(t)$  can then be expressed by

$$\rho_{S+PM}(t) = \sum_i c_i \exp(\lambda_i t) \hat{\rho}_{S+PM,i}. \quad (9)$$

By tracing out these PMs, one can observe that the exact dynamics of the system's reduced state follows a similar expression, replacing these eigenmatrices  $\hat{\rho}_{S+PM,i}$  with the reduced eigenmatrices  $\hat{\rho}_{S,i} = \text{tr}_{PM}(\hat{\rho}_{S+PM,i})$ , namely,

$$\rho_S(t) = \sum_i c_i \exp(\lambda_i t) \hat{\rho}_{S,i}. \quad (10)$$

To describe EPs, one considers a family of parametrized extended Liouvillian superoperators  $\mathcal{L}_{S+PM}(\xi)$ , bearing in mind that  $\xi$  includes the parameters related to both the system and the structured environments. Since  $\mathcal{L}_{S+PM}(\xi)$  is generally non-Hermitian, EPs could potentially exist in the parameter space. For instance, let  $\xi_{EP,n}$  represent an  $n$ th-order EP in the parameter space, where  $n$  different eigenvalues and the corresponding eigenmatrices  $\{\lambda_i, \hat{\rho}_{S+PM,i}\}_{i \in A}$  coalesce into  $\{\lambda_{EP}, \hat{\rho}_{S+PM,\lambda_{EP}}\}$ . Here,  $A$  denotes a set of indices. Due to the coalescence of the eigenmatrices, the corresponding  $n$ -dimensional eigensubspace for  $\mathcal{L}_{S+PM}(\xi_{EP})$  cannot be diagonalized. Nevertheless, a Jordan block for the subspace can be constructed by introducing generalized eigenmatrices  $\{\hat{\rho}_{S+PM,\lambda_{EP}}^{(j)}\}_{j=0, \dots, n-1}$ , such that the system dynamics can be expressed by

$$\rho_S(t) = \sum_{i \notin A} c_i e^{\lambda_i t} \hat{\rho}_{S,i} + e^{\lambda_{EP} t} \sum_{j=0}^{n-1} \sum_{m=0}^j \frac{t^m \tilde{c}_m}{m!} \hat{\rho}_{S,\lambda_{EP}}^{(j)}, \quad (11)$$

where the reduced generalized eigenmatrices are introduced as

$$\hat{\rho}_{S,\lambda_{EP}}^{(j)} = \text{tr}_{PM}(\hat{\rho}_{S+PM,\lambda_{EP}}^{(j)}). \quad (12)$$

Equation (11) suggests that the polynomial time dependence, a common dynamical signature of EPs, could be observed in the reduced dynamics of the open system. In essence, the PMEOM provides an intuitive and direct route to investigate EPs beyond the BMS approximation, and this approach is compatible with the conventional spectral analysis by introducing the (generalized) reduced eigenmatrices.

It is worth noting that an alternative approach is to consider the framework of the HEOM. In this context, a set of ADOs is introduced to capture the non-Markovian and non-perturbative effects<sup>54,56,58,66-68</sup>. Similarly, we can define the extended quantum state  $\rho_{S+ADO}$  that contains both the system-reduced state and the ADOs. The dynamics of the extended state are governed by the extended Liouvillian superoperator  $\mathcal{L}_{S+ADO}$ . The system's reduced state can be obtained through a linear operation, specifically  $\rho_S(t) = \mathcal{P}[\rho_{S+ADO}(t)]$ , where  $\mathcal{P}$  is a superoperator for discarding all the ADOs (see Methods). Therefore, the EPs for non-Markovian open quantum systems can also be

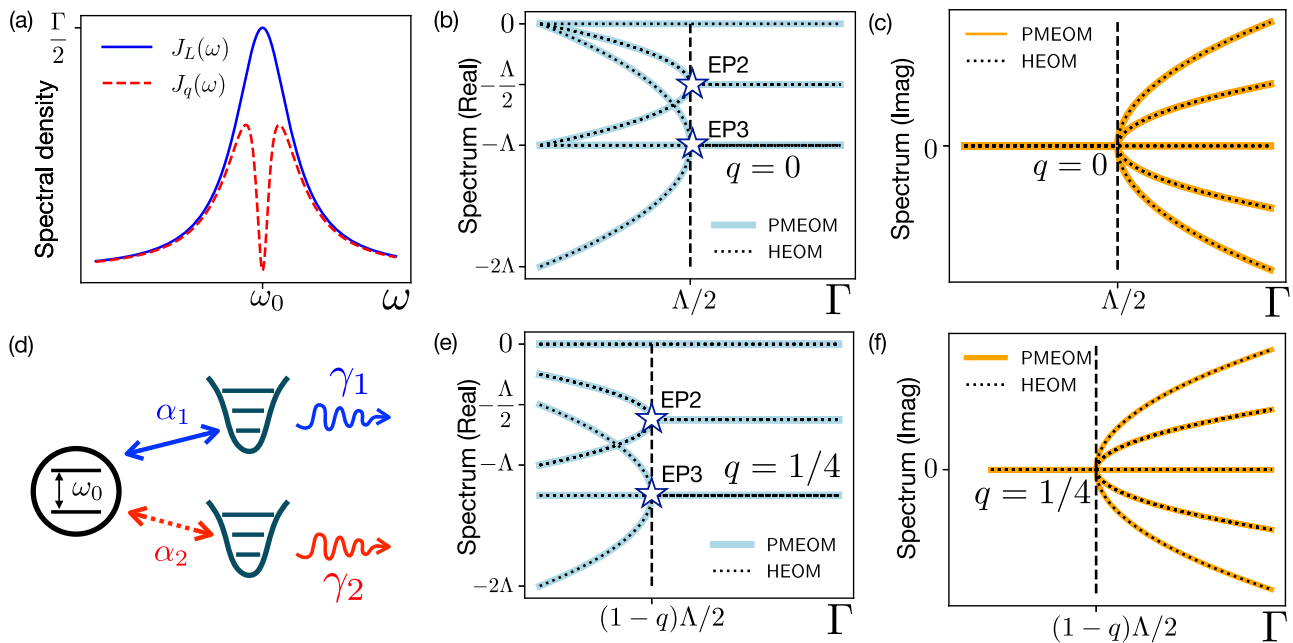


**Fig. 2 | EPs for the spin-boson model.** **a** Lorentzian  $J_L(\omega)$  and band gap  $J_q(\omega)$  spectral densities centered at the qubit transition frequency  $\omega_0$ . **d** The effects of these spectral densities can be represented by two PMs: The Lorentzian spectral density can be described by the upper PM with qubit-PM coupling strength  $\alpha_1 = \sqrt{\Gamma\Lambda/2}$  and PM's damping rate  $\gamma_1 = 2\Lambda$ , while the band gap is characterized by the lower PM with the non-Hermitian coupling  $\alpha_2 = i\sqrt{q\Gamma\Lambda/2}$  and damping rate  $\gamma_2 = 2q\Lambda$ , where the red dashed

line signifies the unphysical nature of this PM. **b, c** The real and imaginary parts of the spectrum of the extended Liouvillian for the gapless scenario ( $q = 0$ ). Two EPs, EP2 and an EP3 emerge at the coupling strength  $\Gamma = \Lambda/2$ . **e, f** The real and imaginary parts of the spectrum of the extended Liouvillian with  $q = 1/4$ . The EP criterion becomes  $\Gamma = (1 - q)\Lambda/2$ . The dotted curves in **b, c, e, f** represent the spectrum of the extended superoperators for HEOM (see Supplementary Information for detailed derivations).

equivalently characterized under the framework of the HEOM by introducing the corresponding (generalized) reduced eigenmatrices, which are expressed as  $\tilde{\rho}_{S,i} = \mathcal{P}(\tilde{\rho}_{S+\text{ADO},i})$  and  $\tilde{\rho}_{S,\Lambda_{\text{EP}}}^{(j)} = \mathcal{P}(\tilde{\rho}_{S+\text{ADO},\Lambda_{\text{EP}}}^{(j)})$ .

**Spin-boson model**

To gain a more intuitive understanding, we apply the PMEOM to the prototype spin-boson model, showing that additional EPs without Markovian analog can be observed by adjusting the structural characteristics of the environment's spectral density. To simplify our analysis, we consider a zero-temperature environment and adopt the rotating-wave approximation (RWA), where the system-environment interaction in Eq. (2) and the system-PM coupling in Eq. (8) can be expressed by  $\sum_k g_k(Qb_k^\dagger + \tilde{Q}^\dagger b_k)$  and  $\sum_i \alpha_i(Qa_i^\dagger + \tilde{Q}^\dagger a_i)$ , respectively. Furthermore, we consider a scenario where the spectral density function  $J(\omega)$  is well localized in the vicinity of a high-frequency  $\omega_0 \gg 0$ , enabling us to effectively approximate the correlation in Eq. (6) by extending the lower limit of the integral to negative infinity. Note that the assumptions mentioned above are also considered in the original proposals of PMEOM<sup>38-40</sup>.

The model involves a qubit representing the open system, where the system Hamiltonian and system-environment coupling operator are  $H_S = \omega_0|e\rangle\langle e|$  and  $\tilde{Q} = \sigma_-$ , respectively. Such an interaction can lead to an energy exchange between the qubit and the environment, thereby inducing non-Hermiticity for the system. Here,  $\omega_0$  denotes the qubit transition frequency between the ground state  $|g\rangle$  and the excited state  $|e\rangle$ , and  $\sigma_+ = |e\rangle\langle g|$  ( $\sigma_- = |g\rangle\langle e|$ ) represents the raising (lowering) operator. We consider a Lorentzian spectral density that is expressed by

$$J_L(\omega) = \frac{1}{2} \frac{\Gamma\Lambda^2}{(\omega - \omega_0)^2 + \Lambda^2}, \tag{13}$$

where  $\Gamma$  and  $\Lambda$  denote the coupling strength and the spectral width, respectively. In the interaction picture and under the earlier specified assumption of extending the spectral density function to negative

frequencies, the environmental correlation function can be expressed by a single exponential term, i.e.,  $C(t) = (\Gamma\Lambda/2) \exp(-\Lambda|t|)$ . Therefore, the PMEOM can be constructed by introducing a single PM with the damping rate  $\gamma = 2\Lambda$  and the qubit-PM coupling strength  $\alpha = \sqrt{\Gamma\Lambda/2}$ . As aforementioned, the PM representation provides a physical intuition that the EP could be located by balancing  $\gamma$  and  $\alpha$  (or  $\Gamma$  and  $\Lambda$ ) so that the system reaches a critical damping point.

The corresponding extended Liouvillian superoperator  $\mathcal{L}_{S+\text{PM}}(\Gamma, \Lambda)$  can be described by a  $9 \times 9$  non-Hermitian matrix in the single-excitation subspace (Supplementary Information). The spectrum is illustrated in Fig. 2, revealing that  $\Gamma = \Lambda/2$  corresponds to a second-order EP (EP2) and a third-order EP (EP3). Notably, these EPs are unobservable in the Markovian wide-band limit. Specifically, in such a limit, the spectral width (and thus the damping rate of the PM) becomes infinite,  $\Lambda \rightarrow \infty$ . Therefore, the PM can be adiabatically eliminated, and the dynamics are governed by a qubit-only Markovian master equation, i.e.,  $\dot{\rho}_S(t) = \Gamma[2\sigma_- \rho_S(t) \sigma_+ - \{\sigma_+ \sigma_-, \rho_S(t)\}]/2$ . Intuitively, there is only one qubit decay channel without internal tunneling between the qubit energy levels, thereby EP does not emerge in this scenario<sup>17</sup>.

Let us proceed with a deeper analysis of the EP dynamical signatures. According to Fig. 2b, c, the EP condition pinpoints a real-to-complex transition in the spectrum. In other words, the EP condition corresponds to a critical damping point, separating the overdamped (pure decay) and underdamped (oscillatory) regimes. By investigating the generalized eigenmatrices for the extended superoperator at the EP condition, i.e.,  $\mathcal{L}_{S+\text{PM}}(\Gamma = \Lambda/2)$ , we conclude that the qubit coherence and population dynamics are respectively determined by the EP2 and EP3, resulting in observing first-order and second-order polynomial time dependencies:

$$\begin{aligned} \langle e|\rho_S(t)|g\rangle &= \frac{1}{2}(\Lambda t + 2)e^{-\frac{1}{2}\Lambda t} \langle e|\rho_S(0)|g\rangle, \\ \langle e|\rho_S(t)|e\rangle &= \frac{1}{4}(\Lambda^2 t^2 + 4\Lambda t + 4)e^{-\Lambda t} \langle e|\rho_S(0)|e\rangle. \end{aligned} \tag{14}$$

Furthermore, the transition from the overdamped to underdamped regimes opens up the possibility of observing enhanced sensitivity to external perturbations in the vicinity of the EP. For instance, consider a small perturbation in the coupling strength, represented as  $\Gamma \rightarrow \Lambda(1 + \epsilon)/2$ , with  $\epsilon > 0$ . This perturbation induces splittings in the imaginary parts of the eigenvalues, resulting in oscillatory dynamics. Notably, these splittings scale as  $\sqrt{\epsilon}$ , indicating the sensitivity enhancement in the characteristic frequency of the oscillatory behavior. For this model, both the qubit excited state population and coherence vanish periodically. We choose, for simplicity, the first vanishing time  $t_{\text{vanish}}$  of the qubit coherence to capture the system's oscillations. One can find  $t_{\text{vanish}}^{-1} \approx \Lambda\sqrt{\epsilon}/2 + O(\epsilon)$ , which implies that  $t_{\text{vanish}}$  is sensitive to external perturbation when the system is prepared at the EP.

Up to this point, we only tune the environmental parameters without changing the shape of the Lorentzian profile, and we have shown that such an adjustment does not modify the structure of the PMEOM. Let us further consider a more complex scenario, where an additional parameter can drastically modify the spectral shape. To this end, we introduce a band-gap structure to the Lorentzian background<sup>31</sup>, which is modeled as

$$J_q(\omega) = J_L(\omega) - \frac{1}{2} \frac{\Gamma(q\Lambda)^2}{(\omega - \omega_0)^2 + (q\Lambda)^2}, \quad (15)$$

where the band gap is located at the frequency  $\omega_0$ , such that  $J_q(\omega_0) = 0$ <sup>31</sup> [see also Fig. 2a], and the parameter  $q \in (0, 1]$  is used to control the relative width for the band gap. The environmental correlation function is now expressed by two exponential terms:

$$C(t) = \frac{\Lambda\Gamma}{2} \exp(-\Lambda|t|) - \frac{q\Lambda\Gamma}{2} \exp(-q\Lambda|t|). \quad (16)$$

Accordingly, the PMEOM for the exact dynamics involves two PMs ( $a_1$  and  $a_2$ ), each characterized by the qubit-PM coupling strengths and PM damping rates [see also Fig. 2d]:  $\{\alpha_1 = \sqrt{\Gamma\Lambda}/2, \alpha_2 = i\sqrt{q}\alpha_1, \gamma_1 = 2\Lambda, \gamma_2 = q\gamma_1\}$ . The spectrum of the corresponding extended Liouvillian superoperator is presented in Fig. 2e, f, suggesting that the EP criterion becomes

$$\Gamma = (1 - q)\Lambda/2. \quad (17)$$

Consequently, including a band gap into the environmental spectral profile leads to a displacement of the EP in the parameter space. In this case, the system requires a smaller coupling strength to reach the EP criterion compared to the case of the previous gapless Lorentzian environment.

We remark that  $\alpha_2$  is purely imaginary, so it does not directly correspond to a physical mode. This characteristic causes the  $H_{S+PM}$  to become non-Hermitian<sup>43</sup>. Nevertheless, the reduced dynamics of the qubit is still exact and well-behaved as long as the PMEOM is consistent with the given  $C(t)$ <sup>43</sup>. Furthermore, in Fig. 2 and Supplementary Information, we demonstrate that the spectrum of the extended Liouvillian operators for the HEOM is consistent with that of PMEOM.

Another notable aspect is that the EP condition also aligns with the onset of non-Markovianity by utilizing the Breuer–Laine–Piilo (BLP)<sup>69</sup> and the Rivas–Huelga–Plenio (RHP)<sup>70</sup> non-Markovianity measures. Specifically, for the spin-boson model, the analytical solution for the qubit-reduced state is expressed as<sup>31</sup>

$$\begin{aligned} \langle e|\rho_S(t)|e\rangle &= \langle e|\rho_S(0)|e\rangle |G(t)|^2, \\ \langle g|\rho_S(t)|e\rangle &= \langle g|\rho_S(0)|e\rangle G(t). \end{aligned} \quad (18)$$

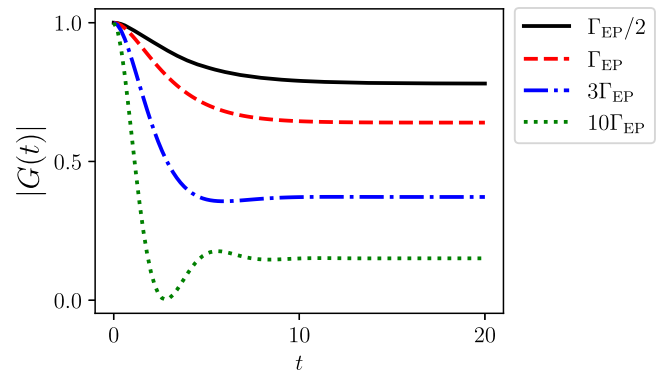


**Fig. 3 | Dynamics of the decoherence function  $|G(t)|$  for different values of the coupling strength  $\Gamma$ .** Here,  $\Gamma_{\text{EP}} = (1 - q)\Lambda/2$ , and we set  $\Lambda = 1$  and  $q = 1/4$ .

Here,  $G(t)$  is commonly referred to as the decoherence function<sup>71</sup>, which is given by

$$G(t) = \frac{\Gamma e^{-\Lambda\delta_+ t/2}}{2q\Lambda - \Gamma\delta_-} \left[ \frac{\delta_+ \sqrt{\Lambda\delta_-} \sinh(\eta t)}{\sqrt{2\Gamma + \Lambda\delta_-}} - \delta_- \cosh(\eta t) \right] + \frac{2q\Lambda}{2q\Lambda - \Gamma\delta_-}. \quad (19)$$

with  $\delta_{\pm} = q \pm 1$  and  $\eta = \sqrt{\Lambda\delta_- (2\Gamma + \Lambda\delta_-)}/2$ . It is well-established that for both the BLP and the RHP measures, the transition from Markovian to non-Markovian dynamics occurs when  $|G(t)|$  shifts from pure decay to oscillatory behavior<sup>71</sup>. Consequently, the transition point can be identified from Eq. (18) as  $\delta_+ \Lambda = -2\Gamma$ , or equivalently  $\Gamma = (1 - q)\Lambda/2$ , precisely aligning with the EP condition in Eq. (17). In Fig. 3, we present the dynamics of the decoherence function  $|G(t)|$  for different values of  $\Gamma$ , where  $\Gamma_{\text{EP}} = (1 - q)\Lambda/2$  corresponds to the EP criterion. One can observe that the dynamics changes from monotonic decay (overdamped) to oscillatory behavior (underdamped), as  $\Gamma$  increases and crosses the EP at  $\Gamma = \Gamma_{\text{EP}}$ .

### Linear bosonic systems with adjoint pseudomode-equation of motion

The PMEOM in Eq. (8) offers significant flexibility by allowing both the system Hamiltonian  $H_S$  and the coupling operator  $Q$  to be arbitrary. This utility facilitates the extension of our analysis to a variety of open quantum systems. As an illustrative application, we now explore linear bosonic systems, which have garnered significant interest in the study of both LEPs and HEPs<sup>11,18,20,21,24</sup>. Specifically, we examine a general Hamiltonian with  $M$  coupled modes, expressed as

$$H_S = \sum_{k=1}^M \Omega_k c_k^\dagger c_k + \sum_{j < k} \chi_{j,k} (c_j^\dagger c_k + c_k^\dagger c_j), \quad (20)$$

where  $\Omega_k$  denotes the frequency associated with the mode  $c_k$ , and  $\chi_{j,k}$  represents the coherent coupling between the modes  $j$  and  $k$ .

In the Heisenberg picture, the dynamics are governed by the following adjoint PMEOM:

$$\begin{aligned} \frac{d}{dt} O_{S+PM}(t) &= i[H_{S+PM}, O_{S+PM}(t)] \\ &+ \sum_i \frac{\gamma_i}{2} \left( 2a_i^\dagger O_{S+PM}(t) a_i - \{a_i^\dagger a_i, O_{S+PM}(t)\} \right), \end{aligned} \quad (21)$$

where  $O_{S+PM}(t)$  denotes an arbitrary operator acting on the joint system,  $S + PM$ . To facilitate the analysis, we define a vector containing the annihilation operators for both the system modes and the PMs:

$$\mathbf{v} = (c_1, \dots, c_M, a_1, \dots, a_i, \dots)^T. \quad (22)$$

Focusing on the amplitudes of these modes, we denote

$$\langle \mathbf{v}(t) \rangle = (\langle c_1(t) \rangle, \dots, \langle c_M(t) \rangle, \langle a_1(t) \rangle, \dots, \langle a_i(t) \rangle, \dots)^T, \quad (23)$$

with  $\langle a(t) \rangle = \text{tr}[a(t)\rho_{S+PM}(0)]$ .

Through the adjoint PMEOM, the dynamics for the amplitudes are determined by the effective NHH

$$H_{\text{eff},S+PM} = H_{S+PM} - i \sum_i \gamma_i a_i^\dagger a_i / 2 = \mathbf{v}^\dagger \mathbf{H}_{\text{eff},S+PM} \mathbf{v}, \quad (24)$$

where  $\mathbf{H}_{\text{eff},S+PM}$  is a matrix representation of the NHH. Specifically, one obtains

$$\langle \dot{\mathbf{v}}(t) \rangle = i \mathbf{H}_{\text{eff},S+PM} \langle \mathbf{v}(t) \rangle, \quad (25)$$

indicating that potential EPs can now be encoded in  $\mathbf{H}_{\text{eff},S+PM}$ .

For a concrete example, we examine a two-mode system with

$$\chi_{1,2} = \chi \text{ and } \Omega_1 = \Omega_2 = \omega_0. \quad (26)$$

Also, we consider one of the modes ( $c_2$ ) is further coupled to a Lorentzian environment in zero temperature, as described in Eq. (13). In the wide-band limit ( $\Lambda \rightarrow \infty$ ), the resulting system-only effective non-Hermitian Hamiltonian within the rotating frame is given by:

$$\mathbf{H}_{\text{eff},S} = \begin{pmatrix} 0 & \chi \\ \chi & i\frac{\Gamma}{2} \end{pmatrix}. \quad (27)$$

The corresponding eigenvalues are  $(i\Gamma \pm \sqrt{16\chi^2 - \Gamma^2})/4$ , indicating the presence of an EP2 if  $|\chi| = \Gamma/4$ , with the degenerate eigenvalue  $i\Gamma/4$ . The dynamics at the EP2 can be derived as:

$$\begin{aligned} \langle c_1(t) \rangle &= e^{-\Gamma t/4} \left[ \langle c_1(0) \rangle + \frac{\Gamma t}{4} (\langle c_1(0) \rangle + i \langle c_2(0) \rangle) \right] \\ \langle c_2(t) \rangle &= \frac{1}{4} e^{-\Gamma t/4} [i \langle c_1(0) \rangle \Gamma t + \langle c_2(0) \rangle (4 - \Gamma t)]. \end{aligned} \quad (28)$$

As expected, the first-order time dependence is observed due to the EP2. With a finite width  $\Lambda$ , the effective Hamiltonian takes the form:

$$\mathbf{H}_{\text{eff},S+PM} = \begin{pmatrix} 0 & \chi & 0 \\ \chi & 0 & \sqrt{\frac{\Gamma\Lambda}{2}} \\ 0 & \sqrt{\frac{\Gamma\Lambda}{2}} & i\Lambda \end{pmatrix}. \quad (29)$$

By matching the coefficients of the characteristic polynomial, an EP3 is identified with the following criteria:

$$\left\{ |\chi| = \frac{\Lambda}{3\sqrt{3}}, \Gamma = \frac{16\Lambda}{27} \right\}, \quad (30)$$

and the degenerate eigenvalue is  $i\Lambda/3$ . In this case, the dynamics is written as:

$$\begin{aligned} \langle c_1(t) \rangle &= \frac{e^{-\Lambda t/3}}{27} \left[ \langle c_1(0) \rangle (\Lambda^2 t^2 + 9\Lambda t + 27) \right. \\ &\quad \left. + \langle c_2(0) \rangle i\sqrt{3}\Lambda t(\Lambda t + 3) \right], \\ \langle c_2(t) \rangle &= \frac{e^{-\Lambda t/3}}{9\sqrt{3}} \left[ \langle c_1(0) \rangle i\Lambda t(\Lambda t + 3) \right. \\ &\quad \left. - \langle c_2(0) \rangle \sqrt{3} (\Lambda^2 t^2 - 3\Lambda t - 9) \right], \end{aligned} \quad (31)$$

where the second-order time dependence can be observed due to the EP3.

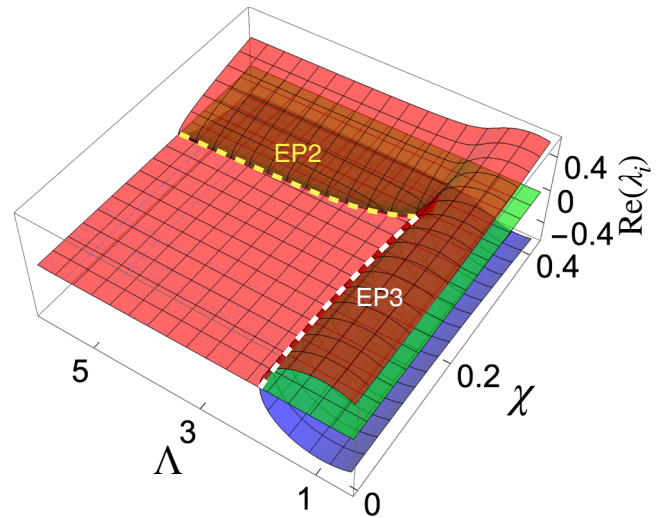


**Fig. 4 | EP2 and EP3 curves for the two-coupled-modes model.** Real part of the eigenvalues  $\lambda_i$  ( $i=1, 2, 3$ ), corresponding to the effective Hamiltonian described in Eq. (29), as a function of the spectral width  $\Lambda$  and coupling strength  $\chi$ . Here, we set  $\Gamma=1$ . The yellow and white dashed curves represent the EP2 and EP3 curves, respectively.

In Fig. 4, we present the real part of the eigenvalues for different values of  $\chi$  and  $\Lambda$ . The EP2 (yellow dashed curve) originates from the prediction in the wide-band limit [i.e., Eq. (27)]. As  $\Lambda$  decreases, one can observe that the EP2 is transformed into the EP3 (white dashed curve) when  $\Lambda$  becomes sufficiently small. This demonstrates that the order of the EP can be upgraded by adjusting the characteristics of the structured environment.

This upgrade can lead to a further enhancement in the system's sensitivity. For instance, we introduce a perturbation  $\epsilon > 0$  to the coupling strength  $\chi \rightarrow \chi(1 + \epsilon)$ . In the vicinity of the EP3, the eigenvalues take the form

$$\left\{ i\frac{\Lambda}{3} + x_1 \Lambda \epsilon^{\frac{1}{3}} + O(\epsilon^{\frac{2}{3}}), i\frac{\Lambda}{3} + x_2 \Lambda \epsilon^{\frac{1}{3}} + O(\epsilon^{\frac{2}{3}}), i\frac{\Lambda}{3} + x_3 \Lambda \epsilon^{\frac{1}{3}} + O(\epsilon^{\frac{2}{3}}) \right\}, \quad (32)$$

where  $x_1$ ,  $x_2$ , and  $x_3$  are constants. We can observe a cubic-root bifurcation for the EP3 in response to the external perturbation, signifying sensitivity enhancement.

Intuitively, one may anticipate that higher-order EPs may emerge when considering an environment with a more complicated spectral structure, which requires more PMs to capture the non-Markovian dynamics and increases the dimension of the non-Markovian NHHs

### Discussion

We have presented a general theory on characterizing non-Markovian EP based on the PMEOM and HOEM. The proposed theory can be viewed as a unified framework for investigating quantum EPs in both the Markovian and non-Markovian regimes, as the PMEOM and HEOM provide exact descriptions of open system dynamics. Moreover, according to the PMEOM and HEOM formalisms, non-Markovian effects can effectively increase the dimensionality of the associated non-Hermitian (super)operator. This suggests that additional or higher-order EPs could emerge by adjusting the characteristics of structured environments. We demonstrate this with the spin-boson and two-coupled-mode models.

A direct extension involves exploring more realistic examples that do not rely on the RWA and restoring the detailed-balance condition<sup>43</sup>. In addition, although this work focuses exclusively on a bosonic environment, the proposed framework can be directly generalized to scenarios with arbitrary combinations of bosonic and fermionic

baths<sup>54,56–58</sup>. Moreover, beyond the PMEOM and HEOM, our method of describing non-Markovian EPs via extended Liouvillian superoperators can also be applied to other pertinent methodologies, such as the dissipation-embedded master equation<sup>72,73</sup> and reaction-coordinate mapping<sup>74–77</sup>.

Future work involves further generalizing the theory of non-Markovian EPs. An intriguing possibility involves extending the hybrid-Liouvillian formalism<sup>19</sup> to the non-Markovian domain by incorporating the postselection of quantum trajectories. Additionally, it is worthwhile to delve into the potential applications emerging from the intricate interplay between the (non-)Markovian exceptional and diabolic points<sup>11,24</sup> or the exotic topology and geometry of the parameter space<sup>78–82</sup>. Such investigations could uncover new aspects of non-Markovian EPs, enhancing our understanding of open quantum systems embedded in environments with memory effects.

## Methods

### Extended Liouvillian superoperators for the HEOM

Here, we introduce the extended Liouvillian superoperators within the HEOM formalism, considering both scenarios with and without the RWA. For the case without the RWA, we decompose the correlation function into exponential terms [as in Eq. (7)]:

$$C(t) = \sum_{u=\mathbb{R}, \mathbb{I}} (\delta_{u, \mathbb{R}} + i\delta_{u, \mathbb{I}}) C^u(t) \quad (33)$$

with  $\mathbb{R}$  and  $\mathbb{I}$  representing real and imaginary parts. Here,  $\delta_{u,v}$  denotes the Kronecker-delta symbol with  $\delta_{\mathbb{R}, \mathbb{R}} = \delta_{\mathbb{I}, \mathbb{I}} = 1$  and  $\delta_{\mathbb{R}, \mathbb{I}} = \delta_{\mathbb{I}, \mathbb{R}} = 0$ , and

$$C^u(t) = \sum_l^{\text{max}} \xi_l^u \exp(-\chi_l^u t). \quad (34)$$

Through iterative time differentiation of the exact dynamics in Eq. (3), the HEOM can be expressed as a time-local differential equation within an expanded space formed by the ADOs<sup>56,58,66,83,84</sup>:

$$\frac{d}{dt} \rho_{S+\text{ADO}}(t) = \mathcal{L}_{S+\text{ADO}} [\rho_{S+\text{ADO}}(t)]. \quad (35)$$

Here, we label the ADOs with a vector  $\mathbf{j} = [j_m, \dots, j_1]$ , linking each ADO to a specific exponential term in the correlation function. The system's reduced density operator and these associated ADOs can then be expressed as  $\rho_{\mathbf{j}}^{(m)}(t)$ , such that

$$\rho_{S+\text{ADO}} = \begin{bmatrix} \rho_{\mathbf{j}}^{(0)}(t) \\ \rho_{\mathbf{j}}^{(1)}(t) \\ \vdots \\ \rho_{\mathbf{j}}^{(m)}(t) \end{bmatrix}, \quad (36)$$

where  $m$  indicates the hierarchical level of the ADOs, with  $\rho_{\mathbf{j}}^{(0)}(t) = \rho_S(t)$  representing the system-reduced density matrix. Consequently, the system-reduced state can be obtained by performing a projector  $\mathcal{P}$  on the  $\rho_{S+\text{ADO}}$ :

$$\begin{bmatrix} \rho_S(t) \\ 0 \\ \vdots \\ 0 \end{bmatrix} = \mathcal{P}[\rho_{S+\text{ADO}}(t)] = \begin{bmatrix} \mathbb{1} & 0 & \dots & 0 \\ 0 & 0 & \dots & 0 \\ \vdots & \vdots & \ddots & \vdots \\ 0 & 0 & \dots & 0 \end{bmatrix} \begin{bmatrix} \rho_{\mathbf{j}}^{(0)}(t) \\ \rho_{\mathbf{j}}^{(1)}(t) \\ \vdots \\ \rho_{\mathbf{j}}^{(m)}(t) \end{bmatrix}, \quad (37)$$

where  $\mathbb{1}$  is the identity matrix with the same dimension as the system-reduced density operator, and all other elements of  $\mathcal{P}$  are zero. Under this expression of the ADOs, the corresponding extended Liouvillian superoperator of the HEOM can be written as<sup>56,58</sup>

$$\begin{aligned} \mathcal{L}_{S+\text{ADO}} [\rho_{\mathbf{j}}^{(m)}(t)] &= \mathcal{L}_0 [\rho_{\mathbf{j}}^{(m)}(t)] - \sum_{r=1}^m \chi_{j_r} \rho_{\mathbf{j}}^{(m)}(t) \\ &\quad - i \sum_j \mathcal{A}_j [\rho_{\mathbf{j}^+}^{(m+1)}(t)] - i \sum_{r=1}^m \mathcal{B}_{j_r} [\rho_{\mathbf{j}_r}^{(m-1)}(t)], \end{aligned} \quad (38)$$

where a multi-index notation is used:  $\mathbf{j}^+ = [j', j_{m'}, \dots, j_1]$ , and  $\mathbf{j}_r^- = [j_m, \dots, j_{r+1}, j_{r-1}, \dots, j_1]$ , and  $\mathcal{L}_0[\cdot] = -iH_S^{\times}$ . The system-environment interaction is encoded in the superoperators  $\hat{\mathcal{A}}_j$  and  $\hat{\mathcal{B}}_j$  that couple the  $m$ th-level bosonic ADOs to the  $(m+1)$ th- and  $(m-1)$ th-levels, respectively. Their explicit expressions are given by

$$\mathcal{A}_j[\cdot] = Q^{\times} \text{ and } \mathcal{B}_j[\cdot] = \delta_{u, \mathbb{R}} \xi_l^{\mathbb{R}} Q^{\times} + i\delta_{u, \mathbb{I}} \xi_l^{\mathbb{I}} Q^{\circ}. \quad (39)$$

Let us now consider the case with the RWA, where the system-environment interaction is written as  $H_{SE} = \sum_k g_k (\hat{Q} b_k^{\dagger} + \hat{Q}^{\dagger} b_k)$ . In this case, we separate the correlation function into the absorption ( $v = +$ ) and emission ( $v = -$ ) components, namely  $C(t) = \sum_{v=\pm} C^v(t)$ , where

$$\begin{aligned} C^+(t) &= \frac{1}{\pi} \int_0^{\infty} d\omega J(\omega) n^{\text{eq}}(\omega) e^{i\omega t} \\ &= \sum_l^{\text{max}} \xi_l^{v=+} \exp(-\chi_l^{v=+} t), \\ \text{and } C^-(t) &= \frac{1}{\pi} \int_0^{\infty} d\omega J(\omega) [n^{\text{eq}}(\omega) + 1] e^{-i\omega t} \\ &= \sum_l^{\text{max}} \xi_l^{v=-} \exp(-\chi_l^{v=-} t). \end{aligned} \quad (40)$$

Here  $n^{\text{eq}}(\omega) = \{\exp[\omega/k_B T] - 1\}^{-1}$  represents the Bose-Einstein distribution with a temperature  $T$ .

The Feynman-Vernon influence functional can be derived<sup>56,58</sup>:

$$\begin{aligned} \hat{\mathcal{F}}[\cdot] &= - \sum_{\bar{v}=\pm} \int_0^t dt_1 \int_0^{t_1} dt_2 \tilde{Q}^{\bar{v}}(t_1)^{\times} \\ &\quad \left\{ C^v(t_1 - t_2) \tilde{Q}^v(t_2)[\cdot] + C^{v^*}(t_1 - t_2)[\cdot] \tilde{Q}^v(t_2) \right\}, \end{aligned} \quad (41)$$

where  $\tilde{Q}^{v=+}(t) = \tilde{Q}^{\dagger}(t)$  and  $\tilde{Q}^{v=-}(t) = \tilde{Q}(t)$ . Also,  $\bar{v}$  represents the opposite sign of  $v$ : If  $v = +$ , then  $\bar{v} = -$ , and vice versa. The corresponding extended Liouvillian superoperator can then be expressed as

$$\begin{aligned} \mathcal{L}_{S+\text{ADO}}^{\text{RWA}} [\rho_{\mathbf{k}}^{(m)}(t)] &= \mathcal{L}_0 [\rho_{\mathbf{k}}^{(m)}(t)] - \sum_{r=1}^m \chi_{k_r} \rho_{\mathbf{k}}^{(m)}(t) \\ &\quad - i \sum_{k'} \mathcal{A}_{k'} [\rho_{\mathbf{k}^+}^{(m+1)}(t)] - i \sum_{r=1}^m \mathcal{B}_{k_r} [\rho_{\mathbf{k}_r}^{(m-1)}(t)], \end{aligned} \quad (42)$$

where the superoperators  $\mathcal{A}_{k'}$  and  $\mathcal{B}_{k_r}$  are modified as follows

$$\mathcal{A}_k[\cdot] = \tilde{Q}^{\bar{v}\times} \text{ and } \mathcal{B}_k[\cdot] = \xi_l^v \tilde{Q}^v[\cdot] - \xi_l^{v^*} [\cdot] \tilde{Q}^v. \quad (43)$$

## References

1. Heiss, W. The physics of exceptional points. *J. Phys. A Math. Theor.* **45**, 444016 (2012).
2. El-Ganainy, R. et al. Non-Hermitian physics and  $\mathcal{PT}$  symmetry. *Nat. Phys.* **14**, 11 (2018).
3. Miri, M.-A. & Alú, A. Exceptional points in optics and photonics. *Science* **363**, 7709 (2019).

4. Özdemir, Ş. K. et al. Parity–time symmetry and exceptional points in photonics. *Nat. Mater.* **18**, 783 (2019).
5. Bender, C. M. & Boettcher, S. Real Spectra in Non-Hermitian Hamiltonians Having  $\mathcal{PT}$  Symmetry. *Phys. Rev. Lett.* **80**, 5243 (1998).
6. Bender, C. M. Making sense of non-Hermitian Hamiltonians. *Rep. Prog. Phys.* **70**, 947 (2007).
7. Mostafazadeh, A. Pseudo-Hermiticity versus PT symmetry: the necessary condition for the reality of the spectrum of a non-Hermitian Hamiltonian. *J. Math. Phys.* **43**, 205 (2002).
8. Peng, B. et al. Loss-induced suppression and revival of lasing. *Science* **346**, 328 (2014).
9. Jing, H. et al.  $\mathcal{PT}$ -Symmetric Phonon Laser. *Phys. Rev. Lett.* **113**, 053604 (2014).
10. Zhang, J. et al. A phonon laser operating at an exceptional point. *Nat. Photon.* **12**, 479 (2018).
11. Arkhipov, I. I. et al. Dynamically crossing diabolic points while encircling exceptional curves: a programmable symmetric-asymmetric multimode switch. *Nat. Commun.* **14**, 2076 (2023).
12. Chen, W., Özdemir, Ş. K., Zhao, G., Wiersig, J. & Yang, L. Exceptional points enhance sensing in an optical microcavity. *Nature* **548**, 192 (2017).
13. Hodaei, H. et al. Enhanced sensitivity at higher-order exceptional points. *Nature* **548**, 187 (2017).
14. Rechtsman, M. C. Optical sensing gets exceptional. *Nature* **548**, 161 (2017).
15. Wiersig, J. Review of exceptional point-based sensors. *Photon. Res.* **8**, 1457 (2020).
16. Kuo, P.-C. et al. Collectively induced exceptional points of quantum emitters coupled to nanoparticle surface plasmons. *Phys. Rev. A* **101**, 013814 (2020).
17. Minganti, F., Miranowicz, A., Chhajlany, R. W. & Nori, F. Quantum exceptional points of non-Hermitian Hamiltonians and Liouvillians: the effects of quantum jumps. *Phys. Rev. A* **100**, 062131 (2019).
18. Arkhipov, I. I., Miranowicz, A., Minganti, F. & Nori, F. Quantum and semiclassical exceptional points of a linear system of coupled cavities with losses and gain within the Scully-Lamb laser theory. *Phys. Rev. A* **101**, 013812 (2020).
19. Minganti, F., Miranowicz, A., Chhajlany, R. W., Arkhipov, I. I. & Nori, F. Hybrid-Liouvillian formalism connecting exceptional points of non-Hermitian Hamiltonians and Liouvillians via postselection of quantum trajectories. *Phys. Rev. A* **101**, 062112 (2020).
20. Arkhipov, I. I., Miranowicz, A., Minganti, F. & Nori, F. Liouvillian exceptional points of any order in dissipative linear bosonic systems: Coherence functions and switching between  $\mathcal{PT}$  and anti- $\mathcal{PT}$  symmetries. *Phys. Rev. A* **102**, 033715 (2020).
21. Arkhipov, I. I., Minganti, F., Miranowicz, A. & Nori, F. Generating high-order quantum exceptional points in synthetic dimensions. *Phys. Rev. A* **104**, 012205 (2021).
22. Khandelwal, S., Brunner, N. & Haack, G. Signatures of Liouvillian exceptional points in a quantum thermal machine. *PRX Quantum* **2**, 040346 (2021).
23. Zhang, J.-W. et al. Dynamical control of quantum heat engines using exceptional points. *Nat. Commun.* **13**, 6225 (2022).
24. Perina Jr, J., Miranowicz, A., Chimczak, G. & Kowalewska-Kudlaszyk, A. Quantum Liouvillian exceptional and diabolical points for bosonic fields with quadratic Hamiltonians: the Heisenberg-Langevin equation approach. *Quantum* **6**, 883 (2022).
25. Han, P.-R. et al. Exceptional entanglement phenomena: non-Hermiticity meeting nonclassicality. *Phys. Rev. Lett.* **131**, 260201 (2023).
26. Zhou, Y.-L. et al. Accelerating relaxation through Liouvillian exceptional point. *Phys. Rev. Res.* **5**, 043036 (2023).
27. Bu, J.-T. et al. Enhancement of quantum heat engine by encircling a Liouvillian exceptional point. *Phys. Rev. Lett.* **130**, 110402 (2023).
28. Khandelwal, S., Chen, W., Murch, K. W. & Haack, G. Chiral Bell-state transfer via dissipative Liouvillian dynamics. *Phys. Rev. Lett.* **133**, 070403 (2024).
29. Abo, S., Tulewicz, P., Bartkiewicz, K., Özdemir, Ş. K. & Miranowicz, A. Liouvillian exceptional points of non-Hermitian systems via quantum process tomography. *N. J. Phys.* **26**, 123032 (2024).
30. Laha, A., Miranowicz, A., Varshney, R. K. & Ghosh, S. Correlated nonreciprocity around conjugate exceptional points. *Phys. Rev. A* **109**, 033511 (2024).
31. Breuer, H.-P. & Petruccione, F. *The Theory of Open Quantum Systems* (Oxford University Press, 2002).
32. Garmon, S. & Ordonez, G. Characteristic dynamics near two coalescing eigenvalues incorporating continuum threshold effects. *J. Math. Phys.* **58**, 062101 (2017).
33. Cheung, H. F. H., Patil, Y. S. & Vengalattore, M. Emergent phases and critical behavior in a non-Markovian open quantum system. *Phys. Rev. A* **97**, 052116 (2018).
34. Garmon, S., Ordonez, G. & Hatano, N. Anomalous-order exceptional point and non-Markovian Purcell effect at threshold in one-dimensional continuum systems. *Phys. Rev. Res.* **3**, 033029 (2021).
35. Sergeev, T., Zyablovsky, A., Andrianov, E. & Lozovik, Y. E. Signature of exceptional point phase transition in Hermitian systems. *Quantum* **7**, 982 (2023).
36. Mouloudakis, G. & Lambropoulos, P. Coalescence of non-Markovian dissipation, quantum Zeno effect, and non-Hermitian physics in a simple realistic quantum system. *Phys. Rev. A* **106**, 053709 (2022).
37. Khandelwal, S. & Blasi, G. Emergent Liouvillian exceptional points from exact principles. Preprint at [arXiv <https://doi.org/10.48550/arXiv.2409.08100>](https://doi.org/10.48550/arXiv.2409.08100) (2024).
38. Garraway, B. M. Nonperturbative decay of an atomic system in a cavity. *Phys. Rev. A* **55**, 2290 (1997).
39. Dalton, B. J., Barnett, S. M. & Garraway, B. M. Theory of pseudomodes in quantum optical processes. *Phys. Rev. A* **64**, 053813 (2001).
40. Mazzola, L., Maniscalco, S., Piilo, J., Suominen, K.-A. & Garraway, B. M. Pseudomodes as an effective description of memory: Non-Markovian dynamics of two-state systems in structured reservoirs. *Phys. Rev. A* **80**, 012104 (2009).
41. Pleasance, G. & Petruccione, F. Pseudomode description of general open quantum system dynamics: non-perturbative master equation for the spin-boson model. Preprint at [arXiv <https://doi.org/10.48550/arXiv.2108.05755>](https://doi.org/10.48550/arXiv.2108.05755) (2021).
42. Tamascelli, D., Smirne, A., Huelga, S. F. & Plenio, M. B. Non-perturbative treatment of non-Markovian dynamics of open quantum systems. *Phys. Rev. Lett.* **120**, 030402 (2018).
43. Lambert, N., Ahmed, S., Cirio, M. & Nori, F. Modelling the ultra-strongly coupled spin-boson model with unphysical modes. *Nat. Commun.* **10**, 3721 (2019).
44. Pleasance, G., Garraway, B. M. & Petruccione, F. Generalized theory of pseudomodes for exact descriptions of non-Markovian quantum processes. *Phys. Rev. Res.* **2**, 043058 (2020).
45. Cirio, M. et al. Pseudofermion method for the exact description of fermionic environments: from single-molecule electronics to the Kondo resonance. *Phys. Rev. Res.* **5**, 033011 (2023).
46. Luo, S., Lambert, N., Liang, P. & Cirio, M. Quantum-classical decomposition of gaussian quantum environments: a stochastic pseudomode model. *PRX Quantum* **4**, 030316 (2023).
47. Cirio, M., Luo, S., Liang, P., Nori, F. & Lambert, N. Modeling the unphysical pseudomode model with physical ensembles: simulation, mitigation, and restructuring of non-Markovian quantum noise. *Phys. Rev. Res.* **6**, 033083 (2024).
48. Menczel, P., Funo, K., Cirio, M., Lambert, N. & Nori, F. Non-Hermitian pseudomodes for strongly coupled open quantum systems: unravelings, correlations and thermodynamics. *Phys. Rev. Res.* **6**, 033237 (2024).



49. Jin, J., Zheng, X. & Yan, Y. Exact dynamics of dissipative electronic systems and quantum transport: hierarchical equations of motion approach. *J. Chem. Phys.* **128**, 234703 (2008).
50. Kreisbeck, C., Kramer, T., Rodriguez, M. & Hein, B. High-performance solution of hierarchical equations of motion for studying energy transfer in light-harvesting complexes. *J. Chem. Theory Comput.* **7**, 2166 (2011).
51. Ma, J., Sun, Z., Wang, X. & Nori, F. Entanglement dynamics of two qubits in a common bath. *Phys. Rev. A* **85**, 062323 (2012).
52. Li, Z. H. et al. Hierarchical Liouville-space approach for accurate and universal characterization of quantum impurity systems. *Phys. Rev. Lett.* **109**, 266403 (2012).
53. Dunn, I. S., Tempelaar, R. & Reichman, D. R. Removing instabilities in the hierarchical equations of motion: exact and approximate projection approaches. *J. Chem. Phys.* **150**, 184109 (2019).
54. Tanimura, Y. Numerically “exact” approach to open quantum dynamics: the hierarchical equations of motion (HEOM). *J. Chem. Phys.* **153**, 020901 (2020).
55. Ikeda, T. & Scholes, G. D. Generalization of the hierarchical equations of motion theory for efficient calculations with arbitrary correlation functions. *J. Chem. Phys.* **152**, 204101 (2020).
56. Cirio, M., Kuo, P. C., Chen, Y. N., Nori, F. & Lambert, N. Canonical derivation of the fermionic influence superoperator. *Phys. Rev. B* **105**, 035121 (2022).
57. Lambert, N. et al. QuTiP-BoFiN: a bosonic and fermionic numerical hierarchical-equations-of-motion library with applications in light-harvesting, quantum control, and single-molecule electronics. *Phys. Rev. Res.* **5**, 013181 (2023).
58. Huang, Y.-T. et al. An efficient Julia framework for hierarchical equations of motion in open quantum systems. *Commun. Phys.* **6**, 313 (2023).
59. Jing, H., Özdemir, Ş. K., Lü, H. & Nori, F. High-order exceptional points in optomechanics. *Sci. Rep.* **7**, 1 (2017).
60. Wang, S. et al. Arbitrary order exceptional point induced by photonic spin-orbit interaction in coupled resonators. *Nat. Commun.* **10**, 832 (2019).
61. Zhong, Q., Kou, J., Özdemir, Ş. K. & El-Ganainy, R. Hierarchical construction of higher-order exceptional points. *Phys. Rev. Lett.* **125**, 203602 (2020).
62. Zhang, S. M., Zhang, X. Z., Jin, L. & Song, Z. High-order exceptional points in supersymmetric arrays. *Phys. Rev. A* **101**, 033820 (2020).
63. Mandal, I. & Bergholtz, E. J. Symmetry and higher-order exceptional points. *Phys. Rev. Lett.* **127**, 186601 (2021).
64. Nakatsukasa, Y., Sète, O. & Trefethen, L. N. The AAA algorithm for rational approximation. *SIAM J. Sci. Comput.* **40**, A1494 (2018).
65. Xu, M., Yan, Y., Shi, Q., Ankerhold, J. & Stockburger, J. T. Taming quantum noise for efficient low temperature simulations of open quantum systems. *Phys. Rev. Lett.* **129**, 230601 (2022).
66. Kuo, P.-C. et al. Kondo QED: the Kondo effect and photon trapping in a two-impurity Anderson model ultrastrongly coupled to light. *Phys. Rev. Res.* **5**, 043177 (2023).
67. Nakamura, K. & Tanimura, Y. Optical response of laser-driven charge-transfer complex described by Holstein-Hubbard model coupled to heat baths: Hierarchical equations of motion approach. *J. Chem. Phys.* **155**, 064106 (2021).
68. Kato, A. & Tanimura, Y. Quantum heat current under non-perturbative and non-Markovian conditions: applications to heat machines. *J. Chem. Phys.* **145**, 224105 (2016).
69. Breuer, H.-P., Laine, E.-M. & Piilo, J. Measure for the degree of Non-Markovian behavior of quantum processes in open systems. *Phys. Rev. Lett.* **103**, 210401 (2009).
70. Rivas, A., Huelga, S. F. & Plenio, M. B. Entanglement and non-Markovianity of quantum evolutions. *Phys. Rev. Lett.* **105**, 050403 (2010).
71. Breuer, H.-P., Laine, E.-M., Piilo, J. & Vacchini, B. Colloquium: non-Markovian dynamics in open quantum systems. *Rev. Mod. Phys.* **88**, 021002 (2016).
72. Yan, Y. Theory of open quantum systems with bath of electrons and phonons and spins: many-dissipator density matrixes approach. *J. Chem. Phys.* **140**, 054105 (2014).
73. Wang, Y. & Yan, Y. Quantum mechanics of open systems: dissipator theories. *J. Chem. Phys.* **157**, 170901 (2022).
74. Iles-Smith, J., Lambert, N. & Nazir, A. Environmental dynamics, correlations, and the emergence of noncanonical equilibrium states in open quantum systems. *Phys. Rev. A* **90**, 032114 (2014).
75. Iles-Smith, J., Dijkstra, A. G., Lambert, N. & Nazir, A. Energy transfer in structured and unstructured environments: master equations beyond the Born-Markov approximations. *J. Chem. Phys.* **144**, 044110 (2016).
76. Restrepo, S., Böhring, S., Cerrillo, J. & Schaller, G. Electron pumping in the strong coupling and non-Markovian regime: a reaction coordinate mapping approach. *Phys. Rev. B* **100**, 035109 (2019).
77. Anto-Sztrikacs, N. & Segal, D. Capturing non-Markovian dynamics with the reaction coordinate method. *Phys. Rev. A* **104**, 052617 (2021).
78. Ding, K., Fang, C. & Ma, G. Non-Hermitian topology and exceptional-point geometries. *Nat. Rev. Phys.* **4**, 745 (2022).
79. Bergholtz, E. J., Budich, J. C. & Kunst, F. K. Exceptional topology of non-Hermitian systems. *Rev. Mod. Phys.* **93**, 015005 (2021).
80. Ju, C.-Y. et al. Einstein’s quantum elevator: Hermitization of non-Hermitian Hamiltonians via a generalized vielbein formalism. *Phys. Rev. Res.* **4**, 023070 (2022).
81. Ju, C.-Y., Miranowicz, A., Chen, Y.-N., Chen, G.-Y. & Nori, F. Emergent parallel transport and curvature in Hermitian and non-Hermitian quantum mechanics. *Quantum* **8**, 1277 (2024).
82. Ju, C.-Y., Huang, F.-H. & Chen, G.-Y. Quantum state behavior at exceptional points and quantum phase transitions. Preprint at [arXiv](https://doi.org/10.48550/arXiv.2403.16503) <https://doi.org/10.48550/arXiv.2403.16503> (2024).
83. Cainelli, M., Borrelli, R. & Tanimura, Y. Effect of mixed Frenkel and charge transfer states in time-gated fluorescence spectra of perylene bisimides H-aggregates: hierarchical equations of motion approach. *J. Chem. Phys.* **157**, 084103 (2022).
84. Ikeda, T. & Tanimura, Y. Probing photoisomerization processes by means of multi-dimensional electronic spectroscopy: the multi-state quantum hierarchical Fokker-Planck equation approach. *J. Chem. Phys.* **147**, 014102 (2017).

## Acknowledgements

This work is supported by the National Center for Theoretical Sciences and National Science and Technology Council, Taiwan, Grant No. NSTC 113-2123-M-006-001. N.L. is supported by the RIKEN Incentive Research Program and by MEXT KAKENHI Grant Nos. JP24H00816 and JP24H00820. A.M. was supported by the Polish National Science Center (NCN) under the Maestro Grant No. DEC-2019/34/A/ST2/00081. F.N. is supported in part by: Nippon Telegraph and Telephone Corporation (NTT) Research, the Japan Science and Technology Agency (JST) [via the CREST Quantum Frontiers program Grant No. 24031662, the Quantum Leap Flagship Program (Q-LEAP), and the Moonshot R&D Grant Number JPMJMS2061], and the Office of Naval Research Global (ONR) (via Grant No. N62909-23-1-2074).

## Author contributions

J.-D.L. and P.-C.K. conceived the research and carried out the calculations, with help from N.L. and A.M., under the supervision of Y.-N.C. Y.-N.C., and F.N. were responsible for integrating different research units. All authors contributed to the discussion of the central ideas and to the paper.

## Competing interests

The authors declare no competing interests.

## Additional information

**Supplementary information** The online version contains supplementary material available at <https://doi.org/10.1038/s41467-025-56242-w>.

**Correspondence** and requests for materials should be addressed to Franco Nori or Yueh-Nan Chen.

**Peer review information** *Nature Communications* thanks the anonymous reviewer(s) for their contribution to the peer review of this work. A peer review file is available.

**Reprints and permissions information** is available at <http://www.nature.com/reprints>

**Publisher's note** Springer Nature remains neutral with regard to jurisdictional claims in published maps and institutional affiliations.

**Open Access** This article is licensed under a Creative Commons Attribution-NonCommercial-NoDerivatives 4.0 International License, which permits any non-commercial use, sharing, distribution and reproduction in any medium or format, as long as you give appropriate credit to the original author(s) and the source, provide a link to the Creative Commons licence, and indicate if you modified the licensed material. You do not have permission under this licence to share adapted material derived from this article or parts of it. The images or other third party material in this article are included in the article's Creative Commons licence, unless indicated otherwise in a credit line to the material. If material is not included in the article's Creative Commons licence and your intended use is not permitted by statutory regulation or exceeds the permitted use, you will need to obtain permission directly from the copyright holder. To view a copy of this licence, visit <http://creativecommons.org/licenses/by-nc-nd/4.0/>.

© The Author(s) 2025